

Synthesis of Na Doped TiO₂ Nano Photocatalysts Film on Its Photoactivity and Hydrophilicity

Mahamasuhaimi Masae*, Pichaya Pitsuwan, Chaturong Pholthawon and Niti Pawanwatcharakorn

Department of Industrial Engineering, Rajamangala University of Technology Srivijaya, Songkhla Campus, Boyang Sub-district, Muang District, Songkhla 90000, Thailand

Lek Sikong and Peerawas Kongsong

Department of Mining and Materials Engineering, Prince of Songkla University Hat Yai Campus, Songkhla 90110, Thailand

Abstract

Na/TiO₂ nanocomposite films with different amounts of Na were prepared using the sol-gel process and were coated onto glass substrates by dipping methods. These composite thin films were calcined at the temperatures of 400 °C for 1 h. The effect of Na doping in TiO₂ composite films on photocatalytic reaction and hydrophilic property was investigated. The phase formation of TiO₂ was characterized by XRD. The morphology of TiO₂ composite films was observed using atomic force microscopy (AFM). The chemical composition of the prepared films was analyzed using FTIR spectrometry. The photoactivity of synthesized films was performed by means of degradation of methylene blue dye solution under UV and visible light irradiation. The hydrophilic property was measured in terms of contact angles of water droplets on the films at room temperature. It was found that Na doping seemed to affect the TiO₂ phase, the crystallinity of the anatase phase and the crystallite size of the composite films. The crystallite size decreased with an increase in Na content which were 3, 5 and 6 mol%. It was found that 6 mol% Na/TiO₂ film, having the smallest crystallite size, showed the highest photocatalytic reaction and that its films provided the most hydrophilic effect. Only the anatase phase was found at the calcination temperature of 400 °C. The high hydrophilic property was mainly related to the high level of OH radicals on its surface. The super-hydrophilicity (at the contact angle equal to zero) of all new doped TiO₂ films were found at room temperature for 15 minutes.

Keywords: sol-gel; photocatalytic reaction; hydrophilic; Na doped TiO₂ films.

1. Introduction

TiO₂ offers many useful functions and features including antifogging and coating on materials such as glass building, glassware, mirrors, automobile windshields, etc. so that these surfaces becomes self-cleaned [1]. In the auto industry, self-cleaning glass is often used because the thin TiO₂ film on the glass can break down organic substances when

exposed to UV light [2]. There are three different crystal structures of TiO₂ compound: anatase, rutile, and brookite. The efficiency of the photocatalytic activity of TiO₂ significantly depends on its crystallite size, surface area, and crystal structure [3]. From what is known in the literature, anatase, the mixture phase of anatase, and rutile are the structures that have shown the

*Correspondence : susumeme1983@yahoo.com

highest level of photocatalytic activity [4, 5]. Anatase with large surface area, high crystallinity and nano-scaled crystallite size exhibits a high level of photocatalytic activity and hydrophilic surfaces. In the process, oxygen atoms are ejected, and oxygen vacancies are created in the ground state. These holes can oxidize the O anions. Water molecules can then occupy these oxygen vacancies to produce adsorbed OH groups, which tend to make the hydrophilic surface. The greater the duration that the surface is illuminated with UV light, the smaller the contact angle for water becomes. Finally, under a moderate intensity of UV light (after 30 min), the contact angle approaches zero, meaning that water has a tendency to spread perfectly across the surface [6]. Mixed oxides have been widely produced through using the sol-gel process to improve the hydrophilic photocatalytic reaction [7]. The modification of titania by doping with alkali and the cooperative actions of doping were investigated to improve the photocatalytic activity. The improvement in both spectral response and the photocatalytic efficiency could be achieved through a combined approach of doping with alkali with some other action. In 2013, Yang et al. [8] demonstrated that the incorporation of Na into TiO_2 could extend the spectral response into a visible region and that the photocatalytic activity was greatly enhanced when it was further loaded with the alkali oxide $\text{Na}(\text{NO}_3)$ [8]. In addition, Panagiotopoulou and Kondarides [9] found that adding a small amount of alkalis ($x = \text{Li}, \text{Na}, \text{K}, \text{Cs}$) to TiO_2 resulted in the reduction of Ti^{4+} surface species and created a new type of sites at the perimeter of the dispersed metal crystallites. These results provide the necessary dual-function sites required for the water–gas shift reaction to proceed. These studies showed that alkalis modification had a strong promotional effect in the performance of TiO_2 . Alkalis modification is often observed in the enhanced

photocatalytic activity and the improvement of visible light absorption. In this work, in order to improve the self-cleaning properties of TiO_2 under visible light irradiation, we prepared the Na/TiO_2 films using the sol-gel dip coating method. Crystallization, surface microstructure and optical properties of the films were characterized. The hydrophilic and photocatalytic properties of the Na/TiO_2 films were investigated. Also, the mechanism for improving the hydrophilic property and photo-activity was discussed.

2. Materials and Methods

2.1 Preparation of Na/TiO_2 thin films

In a typical preparation procedure, titanium (IV) isopropoxide (TTIP, 99.95%, Fluka Sigma-Aldrich) was added drop-wise under vigorous stirring into the mixture solution containing ethanol (99.9%; Merck Germany), 10 ml glacial acetic acid and sodium nitrate $\text{Na}(\text{NO}_3)$ corresponding to different Na/Ti proportions of 3, 5 and 6 mol% and stirred for 60 min at a room temperature. Then, Na/TiO_2 sol was coated on glass substrates ($5 \times 20 \times 0.3 \text{ cm}^3$) by dipping at room temperature. Before coating, the glass substrates were cleaned with ultrasonic for 15 min, then washed with distilled water and dried at 60°C for 15 min. The dipping speed used was fixed at 0.23 mm/s. The coated substrates were dried at 60°C for 30 min and then heated at the temperature of 400°C for 1 h with the heating rate of $10^\circ\text{C}/\text{min}$.

2.2 Materials characterization

The surface morphology of the prepared films was characterized by scanning electron microscopy (SEM, Quanta, FEI) and atomic force microscopy (AFM) Multi-Mode scanning probes Veeco NanoScope IV with a scan area of $5 \times 5 \mu\text{m}^2$. The X-ray thin film diffraction (XRD) patterns were characterized in terms of the phase compositions and the crystallite size using an x-ray diffractometer (XRD) (Phillips X'pert

MPD, Cu-K α). The crystallite size was determined from XRD peaks using the Scherrer equation [10]

$$D = 0.9\lambda / \beta \cos\theta_B \quad (1)$$

where D is the crystallite size, λ is the wavelength of the x-ray radiation (Cu-K α = 0.15406 nm), β is the width at half maximum height, and θ_B is half of the diffraction angle of the centroid of the peak in degree. The FTIR transmittance spectra of the samples were also analyzed in order to confirm the formation of a hydroxyl function group (TiO₂-OH bonds) of the films. The band gap energy value of TiO₂ in the powder form was measured by the UV-Vis-NIR Spectrometer with an integrating sphere attachment (ShimadzuISR-3100 spectrophotometer with BaSO₄ as reference).

2.3 Photocatalytic reaction test and contact angle measurement

The photocatalytic activity of Na/TiO₂ thin films coated on glass substrates was tested by means of photodegradation of a methylene blue (MB) solution with the initial concentration of 1×10^{-5} M as an indicator under the fluorescence light of 110 W. The testing distance between the substrate and a light source was 14 cm. The concentration of the remaining methylene blue was determined using a UV-Vis spectrophotometer. The hydrophilic properties of the films were investigated by measuring the contact angle using a contact angle meter (OCA 15EC).

3. Results and Discussion

3.1 XRD patterns

The XRD patterns of TiO₂ thin films calcined at 400 °C are presented in Fig. 1. It was found that only the anatase phase can be seen at 0, 3, 5 and 6 mol% Na doping in TiO₂. Sodium doping seems to affect the crystal phase and the crystallite size as shown in Fig.1 and Table 1. The optimum crystallinity of the anatase phase was observed at 6 mol% of sodium. According to

the Scherrer formula, the average crystallite sizes of 6 mol% Na doped samples are estimated to be about 16.99 nm. It was shown that the crystallite size of Na doped TiO₂ is in the range of 16–23 nm, which are all smaller than that of the reference pure TiO₂ sample. In addition, the enlarged localized profile of the main (101) Bragg peaks around at 2θ of 25.3°. Fig.1 reveals that the 6 mol% Na doping in the TiO₂ samples has an obviously broader anatase (101) diffraction peak than the samples doped with 3 and 5 mol% Na ions. As listed in Table 1, the FWHM values of 5 and 6 mol% Na doped TiO₂ were 0.393 and 0.472, respectively, which are considered to be small crystallite size values. Furthermore, the calculation results listed in Table 1 also suggest that 5 and 6 mol% Na doped TiO₂ have the smallest crystallite sizes, namely 20.42 and 16.99 nm, respectively. This may be due to the penetration of Na ions into the TiO₂ lattice, or the Na ions are bonded with oxygen onto the TiO₂ surface to form Na oxides. Both of these possibilities would restrict the growth of TiO₂ nanocrystal [11, 12]. These results confirm that a certain amount (e.g. 6 mol%) of sodium doped can efficiently inhibit the anatase crystal growth as seen in Table1. The Na content in the range of 3-6 mol% can promote the formation of the anatase phase.

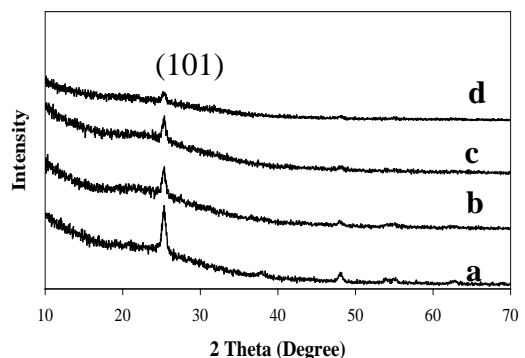


Fig.1. XRD patterns of TiO₂ thin films calcined at 400 °C for 1 h: (a) TiO₂ (b) 3 mol%Na/TiO₂ (c) 5mol%Na/TiO₂ (d) 6mol%Na/TiO₂.

Table1. FWHM, crystallite size, phase composition and photoactivities^a of Na doped TiO₂ and pure TiO₂ samples.

Samples	FWHM (°)	Crystallite size (nm)	Phase content of anatase (%)	Degradation yield (%)
Pure TiO ₂	0.287	29.70	100	42.0
3Na/TiO ₂	0.314	23.18	100	82.5
5Na/TiO ₂	0.393	20.42	100	87.0
6Na/TiO ₂	0.472	16.99	100	90.0

^a Reaction condition: Coated glass substrate (5x20x0.3 cm³) of photocatalyst, 70 ml (1x10⁻⁵) M methylene blue (MB) aqueous solution, a 110 W fluorescence lamp at 14 cm away from the reaction solution, reaction temperature= 25°C, reaction period = 4 h.

3.2 Morphology of surface thin film

The morphology of the coated surface of 6mol % Na/TiO₂ composite thin films synthesized at 400 °C was observed by AFM as illustrated in Fig. 2. The topography fluctuation of the Na/TiO₂ coatings is seen. The average roughness of the 6mol%Na doped TiO₂ composite films is 4.53 nm.

The typical SEM image of as-prepared 6mol%Na doped TiO₂ is shown in Fig. 3. As can be seen from the SEM image, the obtained sample is mainly composed of solid film structure, and some small particles are dispersed on the Na⁺ doped TiO₂ surface. It can be observed that the diameter of the oxide particle ranges from 15 to 25 nm. This follows a similar trend as the XRD analysis shown in Table 1. The energy dispersive spectroscopy mapping of the surface of the 6mol%Na doped TiO₂ sample is shown in Fig. 3. The results show the O and the Ti elements derived from Na/TiO₂ composite photocatalysts. In addition to the above elements, the sodium ions were also detected, indicating that the Na⁺ ions were present in

TiO₂ sample. Na/TiO₂ composite has high photocatalytic activity because of the homogenously high dispersion of nanoTiO₂.

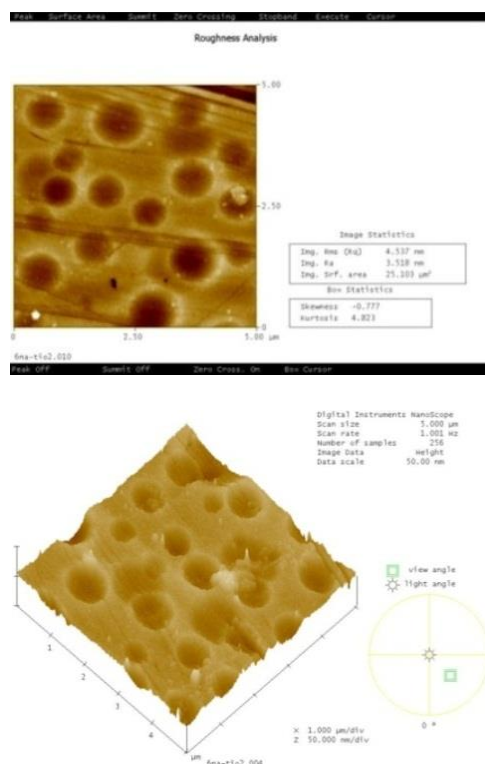


Fig.2. AFM images with a scan area of 5x5 μm² of the 6mol% Na/TiO₂ films calcined at 400 °C.

3.3 FTIR analysis

The photogenerated hydroxyl groups on the titanium dioxide surface can be characterized using FTIR spectroscopy. The FT-IR spectra of representative Na doped TiO₂ and pure TiO₂ samples are shown in Fig. 4. The FT-IR spectra reveal that all the Na doped TiO₂ and the reference TiO₂ sample exhibit absorbance bands in the range of 3700–3100 cm⁻¹ indicating the stretching vibration of -OH or absorbed water molecules [13,14]. The band at 1630 cm⁻¹ was attributed to the bending vibrations of the O-H bond. It has been reported that more hydroxyl groups existing on the titania surface favor the enhancement of the photocatalytic activity [15]. The stronger

absorbance peak around $800\text{--}550\text{ cm}^{-1}$ corresponds to the vibration of Ti–O and the Ti–O–Ti bridging in the stretching modes [13,14,16]. In comparison with the pure TiO_2 , the alkalis doped TiO_2 samples display one extra absorbance peak at 1350 cm^{-1} , which is assigned to the bending vibration band (ν_3) of nitrate [17]. This may be caused by the presence of the nitrate species on the surface of the TiO_2 sample obtained. These results confirm the presence of a hydroxyl group generated by the photocatalytic reaction of the catalyst in the structure of films. The hydroxyl group and the absorbed water are helpful to the photocatalytic reaction and the hydrophilic property since they react with photogenerated holes on TiO_2 surfaces to produce hydroxyl radicals, which are powerful oxidants [18].

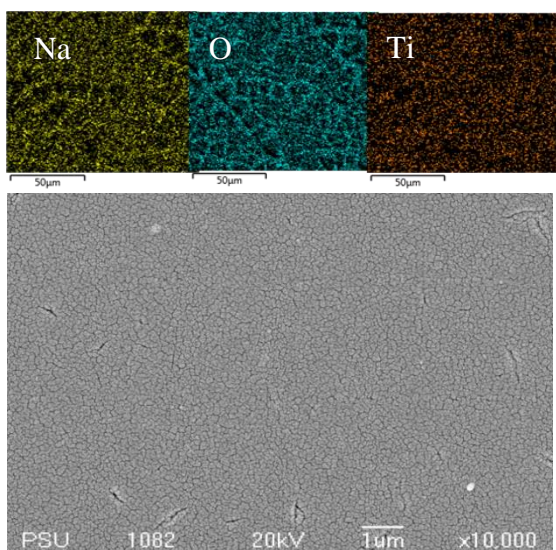


Fig.3. SEM images of the 6mol% Na/ TiO_2 films (inset shows EDS mapping of Na (left), O (middle) and Ti (right)).

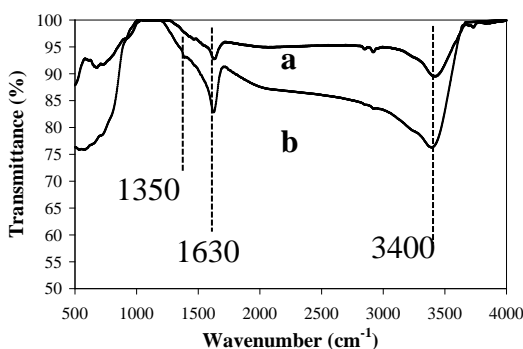


Fig.4. FTIR spectra of Pure TiO_2 (a) and 6mol%Na doped TiO_2 (b) powders calcined at $400\text{ }^{\circ}\text{C}$.

3.4 Photocatalytic activity and hydrophilic property

The photocatalytic activity of the Na doped TiO_2 photocatalytic films was performed by degrading a methylene blue solution (MB) with an initial concentration of $1 \times 10^{-5}\text{ M}$ under fluorescence light irradiation multiple times. It appeared that Na doping had an effect on the photocatalytic activity of the as-prepared samples and that the 6 %mol Na/ TiO_2 thin film exhibited the optimum photoactivity as shown in Fig. 5. According to a previous report [3,5,8,9], many factors influenced the photoactivity of TiO_2 photocatalyst including crystalline phase, grain size, specific surface area, surface morphology and surface state (surface OH radical). These factors were closely related to each other [8,19,20]. As shown in Fig.1 and Table 1, the 6 %mol Na/ TiO_2 thin film exhibited the smallest crystallite size (16.99 nm). Moreover, a suitable amount of Na doping can control the crystallite size of the anatase phase [8] while sodium nitrate dispersed on the surface of TiO_2 could prohibit the recombination of the photo-generated electron-hole pairs and increase photo quantum efficiency [21]. These phenomena promote the photocatalytic activity of the film. Na/ TiO_2 composite seems to exhibit the highest performance at

about 90.0 % for the degradation of an MB solution at 400 °C for 4 h under fluorescence light irradiation (see Fig. 4). Furthermore, Na doping caused a significant formation of OH[•] and O₂ radicals on the photocatalyst surface, resulting in the highest photocatalytic activity under fluorescence light as shown in Fig.5. The results suggest that the photocatalytic activity of Na/TiO₂ photocatalyst is strongly dependent on the amount of Na.

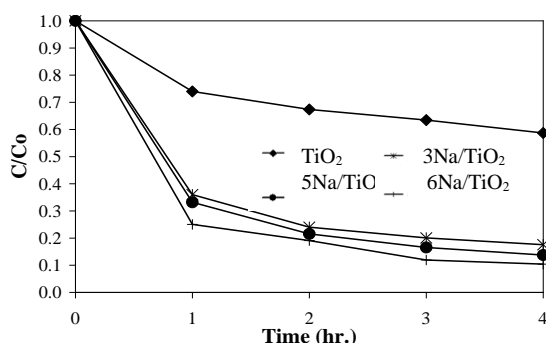


Fig.5. Photocatalytic performance curves of TiO₂ and composite films on degradation of MB under fluorescence light irradiation.

3.5 Energy gap measurement

The UV-vis spectra of pure TiO₂ and composite TiO₂ are shown in Fig. 7. The absorption edge of the samples was determined by the following equation:

$$E_g = 1239.8 / \lambda$$

where E_g is the band gap energy (eV) of the sample and λ (nm) is the wavelength of the onset of the spectrum. It can be seen that most dopants have an effect on the UV-vis spectra due to an inhibition of the recombination of electron-hole pairs [22, 23] especially in the case of 6Na/TiO₂ specimens. The decrease in the optical transition and the long tail is probably caused by lattice defects such as oxygen vacancies [8,20, 23, 24]. From the UV-vis spectra shown in Fig. 7, the band gap energy of the 6

%mol Na doped TiO₂ is shifted by 0.04 eV compared to that of pure TiO₂ (3.20 eV). The band gap energy of 6 %mol Na/TiO₂ was 3.16 eV. These shifts demonstrate how photocatalytic activity may be modulated by atomic-level doping of a nanocatalyst. The absorption wavelength of the 6Na/TiO₂ photocatalyst is extended toward visible light ($\lambda = 392.3$ nm) relative to the other samples [8], giving it the highest photocatalytic activity.

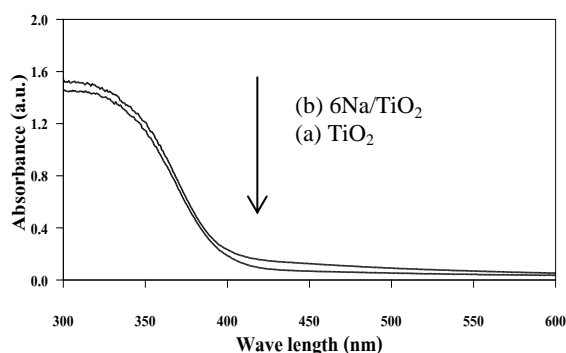


Fig.7. UV-vis diffuse reflectance spectra of (a) pure TiO₂ and (b) 6Na/TiO₂ samples calcined at 400 °C.

The contact angle seems to depend on the photocatalytic activity of the film. It can be noted that the hydrophilicity in terms of contact angle correlates to the photocatalytic activity of the film. The smaller contact angle is responsible for more hydrophilicity. This result agrees well with the finding of Guan [1]. Contact angles and their images of films were done in room temperature as a function of treatment time as shown in Fig. 6. It was found that contact angles decreased with an increase in time and those for 15-minute intervals tended to be small. This is due to the photocatalytic effect of TiO₂ films. Na doping has a significant effect on lowering the contact angle of water droplet due to their enhancement of photocatalytic activity, leading to a high hydrophilic property of the film compared to that of the pure TiO₂ film. The Na doped films of 6 mol % has a smaller

contact angle than the film with lower Na dosage. However, the super-hydrophilicity (contact angle = 0 degree) of all TiO_2 composite films was found after 15 minutes. The 6Na/ TiO_2 films showed the higher

hydrophilic effect than the other Na dosages doped due to their higher degree of anatase crystallinity and the formation of OH^\cdot and O_2^\cdot radicals on the photocatalyst surface.

















Samples	Contact angles images at various observed times			
	0 min	5 min	10 min	15 min
Pure TiO_2				
	97°	78°	70°	55°
3Na/ TiO_2				
	26°	10°	3°	0°
5Na/ TiO_2				
	24°	8°	1°	0°
6Na/ TiO_2				
	21°	5°	0°	0°

Fig.6. Water contact angles and their images of pure TiO_2 and Na/ TiO_2 composite films observed at 0, 5, 10 and 15 minutes.

4. Conclusion

The sodium doped TiO_2 photocatalyst thin films prepared using the sol-gel process exhibit a higher photoactivity than pure TiO_2 films. It was also verified that the high amount of doped Na promotes the formation of basic sites on the surface of TiO_2 . The activity of photocatalyst increased with increasing doped Na amount especially at a low calcination temperature of 400 °C. The synergistic effects of sodium doping with a suitable amount of sodium are responsible for the high photoactivity and the hydrophilic

properties of these TiO_2 composite films due to their smaller crystallite size and the retardation of photo-generated electrons and holes recombination. The 6Na/ TiO_2 films seem to exhibit the optimum photocatalytic reaction, and all of the TiO_2 composite films showed the super hydrophilic property at 15 minutes.

5. Acknowledgements

This investigation was supported by the Thailand Research Fund (RDG5650073). We would like also to acknowledge the

Department of Industrial Engineering, Faculty of Engineering, Rajamangala University of Technology Srivijaya, Songkhla, Thailand and Materials Engineering Research Center (MERC), Faculty of Engineering, Prince of Songkla University for their facility supports.

6. References

- [1] Guan, K., Relationship between photocatalytic activity, hydrophilicity and self-cleaning effect of $\text{TiO}_2/\text{SiO}_2$ films, *Surf. Coat. Tech.*, Vol. 191, pp. 155–160, 2005.
- [2] Hata, S., Kai, Y., Yamanaka, I., Oosaki, H., Hirota, K., and Yamazaki, S. Development of hydrophilic outside mirror coated with titania photocatalyst, *JSAE Review.*, Vol 21, pp.97-102, 2000.
- [3] Nakamura, T., Ichitsubo, T., Matsubara, E., Muramatsu, A., Sato, N., and Takahashi, H. On the preferential formation of anatase in amorphous titanium oxide film, *Scripta Materialia.*, Vol. 53, pp. 1019–1023, 2005.
- [4] Yang, J., Li, D., Wang, X., Yang, X., and Lu, L. Rapid synthesis of nanocrystalline $\text{TiO}_2/\text{SnO}_2$ binary oxides and their photo induced decomposition of methyl orange, *J. Solid State chem.*, Vol. 165, pp. 193 – 198, 2002.
- [5] Zhang, Y., and Reller, A. Phase transformation and grain growth of doped nanosized titania. *Mater. Sci. Eng.*, Vol. 19, pp. 323–326, 2002.
- [6] Hong, W.J. and Kang, M. The super-hydrophilicities of Bi– TiO_2 , V– TiO_2 , and Bi–V– TiO_2 nano-sized particles and their benzene photodecompositions with H_2O addition, *Mater. Lett.*, Vol. 60, pp. 1296–1305, 2006.
- [7] Zhou, F., Kaiming, L., Guoliang, W., Hua, S., and Anmin, H. Crystallization behavior of Li^+ -doped $\text{SiO}_2\text{--TiO}_2$ films prepared by sol–gel dip coating, *J. Cryst. Growth.*, Vol. 264, pp. 297–301, 2004.
- [8] Yang, G., Yan, Z., Xiao, T., and Yang, B. Low-temperature synthesis of alkalis doped TiO_2 photocatalysts and their photocatalytic performance for degradation of methyl orange, *J. Alloy Compd.*, Vol. 580, pp. 15–22, 2013.
- [9] Panagiotopoulou, P., and Kondarides, D.I. Effects of alkali promotion of TiO_2 on the chemisorptive properties and water–gas shift activity of supported noble metal, catalysts *J. Catal.* Vol. 267, pp.57–66 ,2009.
- [10] Qin, H., Gu, G., and Liu, S. Preparation of nitrogen-doped titania with visible-light activity and its application, *C.R. Chimie.*, Vol. 11, pp. 95-100, 2008.
- [11] Bessekhoud, Y., Robert, D., Weber, J.V., and Chaoui, N. Effect of alkaline-doped TiO_2 on photocatalytic efficiency, *J. Photochem. Photobiol. A:Chem.*, Vol. 167, pp. 49–57, 2004.
- [12] Lopez, T., Hernandez-Ventura, J., Gomez, R., Tzompantzi, F., Sinchez, E., Bokhimi, X., and Garcia, A. Photodecomposition of 2,4-dinitroaniline on Li/TiO_2 and Rb/TiO_2 nanocrystallite sol–gel derived catalysts, *J. Mol. Catal. A: Chem.*, Vol. 167, pp. 101–107, 2001.
- [13] Yang, G., Jiang, Z., Shi, H., Jones, M.O., Xiao, T., Edwards, P.P., and Yan, Z. Study on the photocatalysis of F–S co-doped TiO_2 prepared using solvothermal method, *Appl. catal. B:Environ.*, Vol. 96, pp. 458–465, 2010.
- [14] Yang, G., Xiao, T., Sloan, J., Li, G., and Yan, Z. Low-Temperature Synthesis of Visible-Light Active Fluorine/Sulfur Co-doped Mesoporous

- TiO₂ Microspheres, *Chem. Eur. J.*, Vol.17, pp. 1096–1100, 2011.
- [15] Fresno, F., Hernandez-Alonso, M.D., Tudela, D., Coronado, J.M., and Soria, J. Photocatalytic degradation of toluene over doped and coupled (Ti,M)O₂ (M= Sn or Zr) nanocrystalline oxides: Influence of the heteroatom distribution on deactivation, *Appl. Catal. B: Environ.*, Vol. 84, pp. 598–606, 2008.
- [16] Huo, Y., Jin, Y., Zhu, J., and Li, H. Highly active TiO_{2-x-y}N_xF_y visible photocatalyst prepared under supercritical conditions in NH₄F/EtOH fluid, *Appl. Catal. B Environ.*, Vol. 89, pp. 543–550, 2009.
- [17] Linker, R., Shmulevich, I., Kenny, A., and Shaviv, A. Soil identification and chemometrics for direct determination of nitrate in soils using FTIR-ATR mid-infrared spectroscopy, *Chemosphere.*, Vol. 61, pp. 652–658, 2005.
- [18] Lv, K., Zuo, H., Sun, J., Deng, K., Liu, S., Li, X., and Wang, D. (Bi, C and N) codoped TiO₂ nanoparticles, *J. Hazardous Mater.*, Vol. 161, pp. 396–401, 2009.
- [19] Zhao, W., Ma, W.H., Chen, C.C., Zhao, J.C., and Shuai, Z.G. Efficient degradation of toxic organic pollutants with Ni₂O₃/TiO_{2-x}B_x under visible irradiation, *J. Am. Chem. Soc.*, Vol. 126, pp. 4782–4783, 2004.
- [20] Chen, D., Yang, D., Wang, Q., and Jiang, Z. Effects of boron doping on photocatalytic activity and microstructure of titanium dioxide nanoparticles, *Ind. Eng. Chem. Res.*, Vol. 45, pp.4110–4116, 2006.
- [21] Yanagisawa, K. and Ovenstone, J. Crystallization of anatase from amorphous titania using the hydrothermal technique: effects of starting material and temperature, *J. Phys. Chem. B.*, Vol. 103, pp. 7781–7787, 1999.
- [22] Zhang, D. Synthesis and characterization of ZnO-doped cupric oxides and evaluation of their photocatalytic performance under visiblelight, *Transition Met. Chem.*, Vol.35, pp.689–694, 2010.
- [23] Zhang, D. and Zeng, F. Structural, photochemical and photocatalytic properties of zirconium oxide doped TiO₂ nanocrystallites, *Appl.Surf.Sci.*, Vol. 257, pp. 867–871, 2010.
- [24] Kako, T. Zou, Z.G. Katakiri, M. and Ye, J.H. Decomposition of organic compounds over NaBiO₃ under visible light irradiation, *Chem.Mater.*, Vol. pp. 19, 198–202, 2007.